

# Visualizing And Quantifying Lipid Droplets For A Fundamental Understanding Of Non-Alcoholic Fatty Liver Disease

In two-dimensional monolayer and three-dimensional heterospheroid hepatocyte cultures

S. Wissink

Supervisors

*Dr. C. Otto*

*Dr. R. Bansal*

Daily supervisors

*Ing. A.T.M. Lenferink*

*MSc. M.M. Ten Hove*

External committee

*Dr. Ir. N. Bosschaart*



UNIVERSITY OF TWENTE. | TECHMED CENTRE

# **Visualizing And Quantifying Lipid Droplets For A Fundamental Understanding Of Non-Alcoholic Fatty Liver Disease**

In two-dimensional monolayer and three-dimensional heterospheroid hepatocyte  
cultures

**Stan Wissink**

Biomedical Technology BSc

**Bachelor thesis**

**UNIVERSITY  
OF TWENTE.**

Medical Cell BioPhysics / Translational Liver Research  
University of Twente

January 13, 2022

# LIST OF ACRONYMS

NAFLD	Non-Alcoholic Fatty Liver Disease
NASH	Non-Alcoholic Steatohepatitis
TAGs	Triacylglycerols
VLDL	Very-low-density-lipoprotein
DNL	De Novo Lipogenesis
LDs	Lipid droplets
FAs	Fatty acids
PA	Palmitic acid
D-PA	Deuterated-palmitic acid
HCC	Hepatocellular carcinoma

# ABSTRACT

Non-Alcoholic Fatty Liver Disease (NAFLD) is one of the most prevalent liver diseases, affecting more than 25% of the population, and is increasingly common. Early stages of NAFLD are reversible but due to the lack of symptoms, it often leads to irreversible stages where the liver is heavily damaged, before being diagnosed. Eventually, a liver-donor is needed since there is no treatment for these irreversible stages. NAFLD is caused by an excessive amount of fat (steatosis) in hepatocytes (liver cells) in the form of lipid droplets (LDs). LDs are formed when hepatocytes are exposed to fatty acids (FAs). FAs are one of the main sources of energy and energy storage in the human body, about 30% resides from human diet.

In this study, two different FAs, palmitic acid (PA) and deuterated-palmitic acid (D-PA) are tested and compared in different protocols on their ability to induce steatosis in the hepatic progenitor cell line HepaRG and the immortalized human liver carcinoma cell line HepG2. A quantification method is being developed to analyze histological images and quantify the amount of LDs, that are formed upon exposure of FAs, in the hepatocytes. Furthermore, the metabolic activity of the cells is measured to determine the influence of FAs on cell viability. The cells are not only analyzed in two-dimensional monocultures, but also in three-dimensional heterospheroids, since these organoids represent the physical micro-environments inside the human body to a much further extend. Different protocols are used to see if there is a simple way to use spheroids in NAFLD research.

Results showed that cells exposed upon FAs always ended up with more LDs than control cells. D-PA resulted in slightly less LDs overall compared to PA, although this difference was expected. Depending on the cell line and dissolvent used, sometimes higher molarities of FAs resulted in more LDs and sometimes it resulted in less LDs inside the cells. When LD quantification results are compared to metabolic activity, there seems to be a negative correlation between the two: When the number of LDs goes up, the metabolic activity goes down (and vice versa). Not corresponding to literature is the lack of lipotoxicity (cell death due to excessive amount of lipids inside) upon exposure of high concentrations of FAs. Spheroids proved to be very tricky when conducting experiments; metabolic activity signals were too low to have any meaningful value and histological stainings proved un-quantifiable using the created quantification algorithm.

# CONTENTS

<b>List of acronyms</b>	<b>1</b>
<b>Abstract</b>	<b>2</b>
<b>1 Introduction</b>	<b>5</b>
1.1 Non-Alcoholic Fatty Liver Disease	5
1.2 Fatty acids	5
1.2.1 beta-oxidation	6
1.3 Lipid droplets and lipotoxicity	6
1.4 Palmitic acid	7
1.4.1 Deuterated palmitic acid	7
1.5 Hepatic model	7
1.6 Aim of the thesis	7
1.6.1 Approach	8
1.7 Hypothesis	8
<b>2 Materials and methods</b>	<b>9</b>
2.1 Cell cultivation	9
2.2 Induction of lipid droplets in hepatocytes	9
2.3 Monolayer experiments	9
2.4 Lipid droplet quantification	10
2.5 Spheroid formation	11
<b>3 Results and discussion</b>	<b>13</b>
3.1 Cellular metabolic activity	13
3.1.1 HepaRG metabolic activity	13
3.1.2 HepG2 metabolic activity	13
3.1.3 Discussion of cellular metabolic activity	14
3.2 Histological lipid droplet analysis	14
3.2.1 HepaRG	15
3.2.2 HepG2	16
3.2.3 Discussion	17
3.3 Quantification of lipid droplets	18
3.3.1 Discussion of quantification	20
3.4 Spheroid analysis	21
3.4.1 Histological analysis of spheroids	21
3.4.2 Metabolic activity of spheroids	21
3.4.3 Discussion of spheroid analysis	22
<b>4 Conclusion</b>	<b>23</b>

<b>5 Future research</b>	<b>24</b>
<b>References</b>	<b>25</b>
<b>A Oil-Red-O quantification using MATLAB</b>	<b>27</b>

# 1 INTRODUCTION

## 1.1 Non-Alcoholic Fatty Liver Disease

Today, Non-Alcoholic Fatty Liver Disease (NAFLD) is one of the most prevalent liver diseases. Numbers from 2015 show that the group of diseases affects more than a quarter of the worldwide population [1] and is increasingly common.

NAFLD exist on a wide spectrum of disease progression, shown in figure 1.1.

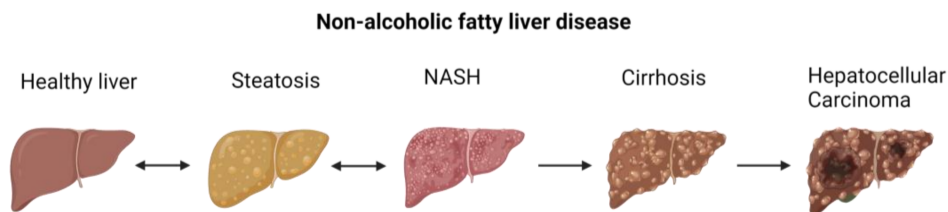


Figure 1.1: Disease progression of Non-Alcoholic Fatty Liver Disease (NAFLD). Steatosis and later Non-Alcoholic Steatohepatitis (NASH) are both reversible. However, when this persists to occur, this leads to liver cirrhosis and eventually hepatocellular carcinoma. [2]

When an excess amount of lipid droplets accumulate inside hepatocytes (liver cells), it is known as NAFLD, when this is not induced or contributed by significant alcohol consumption, autoimmune diseases or viral infections. NAFLD is defined as the presence of at least 5% hepatic steatosis. It can be comprised of simple steatosis or more advanced non-alcoholic steatohepatitis (NASH), which is characterized by inflammation and hepatocyte injury that is often accompanied by fibrosis. Of all people with NAFLD, around 20% of them have NASH.

Since NAFLD is an important cause of chronic liver disease, prevention and early recognition of NAFLD will significantly reduce the need for already scarce liver-donors.

## 1.2 Fatty acids

One of the main sources of energy and energy storage in the human body is in the form of fatty acids (FAs) [3]. All FAs have carboxyl groups at one end of the molecule and long hydrocarbon tails at the other end. This property makes them amphipatic, since the hydrocarbon tail is hydrophobic and the carboxyl group is hydrophilic. There exist over a hundred different kinds of fatty acids. When a FA has no double bonds, they are called saturated fatty acids, otherwise they are called unsaturated fatty acids [4].

The role of fatty acids in the human body is to act as a food reserve in cells. When compared to the weight of glucose, when fatty acids are broken down they can produce as much as six times more energy. Fatty acids can be stored in the cytoplasm of cells in the form of lipid droplets. FAs play an essential role in NAFLD [5].

Around 15-30% of FAs reside from diet and endogenous sources, namely *de novo lipogenesis* (DNL) which accounts for around 30% of FAs. DNL is a very complex pathway that is highly regulated [6]. Under healthy conditions, excess carbohydrates are converted into fatty acids. Later, these FAs are esterified to store triacylglycerols (TAGs). These TAGs could later provide energy via  $\beta$ -oxidation. This pathway is mainly active in the liver and adipose tissue. In a healthy liver, these different mechanisms and pathways are strictly regulated by the liver to maintain a healthy balance of lipid droplet formation and oxidation (figure 1.2). In cancer cells, the DNL-pathway is known to be upregulated and therefore producing more lipids than usual [7].

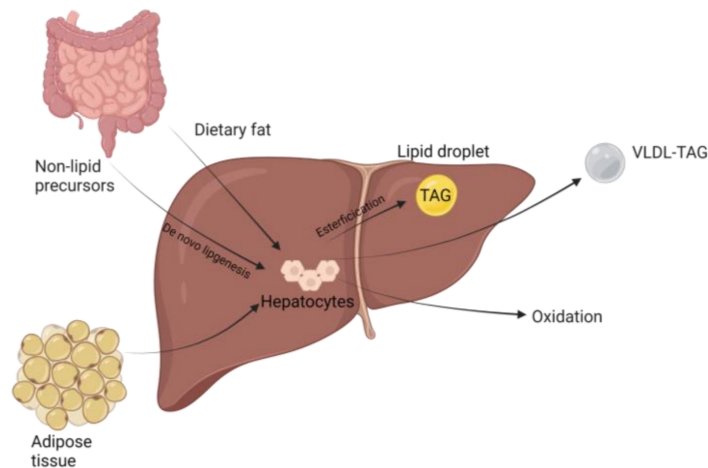


Figure 1.2: Fatty acid metabolism under healthy conditions. Fatty acids inside the liver reside from dietary fat, non-lipid precursors through *de novo lipogenesis* and from nearby adipose tissue. FAs can be stored in the liver as lipid droplets or exit through  $\beta$ -oxidation or as Very-Low Density-Lipoproteins (VLDL-TAG).[2]

### 1.2.1 beta-oxidation

$\beta$ -oxidation is the initial phase of fatty acid oxidation. It occurs in the mitochondria of the cells. Fatty acid chains are broken apart into two-carbon acetic acid fragments. Each acetic acid molecule is fused to coenzyme A, forming acetyl CoA. This molecule enters the citric acid cycle where it is oxidized to  $CO_2$  and  $H_2O$  [8].

### 1.3 Lipid droplets and lipotoxicity

Lipid droplets are formed in the endoplasmic reticulum of the cells and after formation are released into the cytosol [9]. They have a unique structure, where the core consists of neutral lipids which are encircled by a phospholipid monolayer. They can be found in most cells but their presence varies highly between cell types and even individual cells. This difference in presence is due to different metabolic states of individual cells. Overall, the mechanisms of lipid droplet formation is poorly understood [10].

Lipids play a key role in the building of cellular membranes and cell signalling and can be stored in the form of lipid droplets. However, an excessive amount of LDs, in NAFLD often formed by an excessive amount of FAs in the diet, deregulates different pathways, such as unfolded protein response, and can therefore be toxic to cells and eventually induce cell death [10]. Although high amounts of LDs are thought to be related to lipotoxicity, it is also believed that by grouping many free fatty acids together, it can reduce the chance of lipotoxicity.

In general, lipotoxicity refers to the toxic effect that lipids have on cells when present in high numbers, therefore disrupting cell functions and inducing apoptosis (programmed cell death). A commonly used model for lipotoxicity is relatively high doses of palmitic acid, which increases TAG synthesis [9]. The mechanism by which lipotoxicity causes cell-death and -dysfunction is not well understood.

## 1.4 Palmitic acid

Palmitic acid (PA) is the most common circulating fatty acid in the human diet and blood. It does not come as a surprise that therefore, PA is also found to be the most common free FA found in NAFLD patients [11]. PA is a saturated FA since there are no double bonds in the molecule. High concentration of PA or other fatty acids inside non-adipose tissue, in this case liver cells, can induce lipotoxicity[12][13].

### 1.4.1 Deuterated palmitic acid

Another form of PA is deuterated palmitic acid (D-PA). In this molecule, all the hydrogen atoms are substituted by the heavier isotope, deuterium. D-PA is an interesting form of PA since it can be distinguished from other fatty acids using Raman spectroscopy, a very promising technique to identify different molecules, especially in NAFLD research. An interesting phenomenon to note here is the kinetic isotope effect. This effect states that when atoms of a molecule are substituted with heavier isotopes, their reaction or metabolism rate decreases.

## 1.5 Hepatic model

To get a better understanding of lipid droplet formation in NAFLD, there is a need for a good hepatic model for *in vitro* studies. Two well-known hepatocyte cell lines to use in this type of studies are the HepaRG and HepG2 cell line. The HepaRG cell line is a human hepatic progenitor cell line, able to give rise to differentiated hepatocytes. HepaRG cells are known for maintaining significant levels of hepatocyte functions [14]. HepG2 is an immortalized human liver carcinoma cell line which is derived from a 15-year-old caucasian male with hepatocellular carcinoma. The HepG2 cell line is most commonly used for drug metabolism and toxicity studies. A possible downside of these hepatocyte-like cell lines is the potential loss of liver-specific function and enzyme activities.

Culturing a monolayer of these cell lines is a well-known and easy way to create an *in vitro* hepatic model for NAFLD studies. However, monolayers of cells are far from the physiological *in vivo* conditions. A potential better way to approach these conditions as close as possible, is by creating three-dimensional spheroids of cells [15]. Hepatic spheroids represent the heterogeneous cell-to-cell interactions in a much more accurate way. New *in vitro* models that mimic liver complexity and better simulate the complicated pathophysiology of NAFLD and NASH have a very big potential in generating a much better understanding of these increasingly common diseases.

## 1.6 Aim of the thesis

Since there is little known about the formation and distribution of lipid droplets, the aim of this thesis is to visualize and quantify the size and distribution of lipid droplets in human hepatocytes with and without treatment with free fatty acids. To achieve the aim of this thesis, the following objectives were developed:

1. Culturing two-dimensional monocultures and three-dimensional heterospheroids to visualize and quantify lipid droplets using Oil-Red-O stainings and image analysis.
2. Performing an Alamar Blue assay on two-dimensional and three-dimensional cultures to estimate cell viability.

### 1.6.1 Approach

To approach these different objectives, two different concentrations of palmitic acid are added to induce fat overload and compare the effect of different molarities and see if higher molarities lead to possible lipotoxicity. Furthermore, deuterated-PA is compared to protonated-PA to study possible differences in lipid droplet formation. PA and D-PA are dissolved in either ethanol or isopropanol, to determine which dissolvent works best. All those different conditions are tested on two human hepatocyte cell lines: HepG2 and HepaRG in a two-dimensional monolayer to determine the best model for lipid droplet formation. Furthermore, three-dimensional heterospheroids are cultured to investigate their potential in NAFLD studies.

## 1.7 Hypothesis

It is expected that lipid droplets are formed in both hepatocytes cell lines upon exposure of PA as well as D-PA, although D-PA is expected to induce lower amounts of LDs due to the lower metabolic activity by the kinetic isotope effect.

Also, higher molarities of fatty acids are expected to result in lipotoxicity in the cells, which will translate into a lower cell viability. The progenitor cell line HepaRG is expected to be closer to the clinical *in vivo* environment compared to the HepG2 cell line since HepG2 is a carcinoma cell line. This makes the HepaRG cell line possibly a more suitable model for *in vitro* NAFLD studies.

Finally, it is expected that three-dimensional heterospheroids mimic the physical micro-environments more closely as apposed to monolayer cellcultures, although spheroids are known for their difficulties and limitations when performing experiments in the laboratory.

## 2 MATERIALS AND METHODS

### 2.1 Cell cultivation

As mentioned before, two human hepatocyte cell lines are used. They are both cultured in an incubator at 37 °C at 5%  $CO_2$  levels.

#### HepaRG

HepaRG is a human hepatic progenitor cell line with the ability to differentiate into hepatocytes. The cells were differentiated hepatocytes<sup>1</sup> (Differentiated-HepaRG cells) by receiving a 14 day dimethyl sulfoxide (DMSO) treatment. The cells were cultured in a T75 culture flask in Williams E medium, containing 10% heat-inactivated Fetal Bovine Serum (FBS), 1% L-Glutamine (Lonza), 1% Penicillin/Streptomycin (Lonza), 5 µg/ml Insulin (Sigma-Aldrich) and 0.36% hydrocortisone (Sigma-Aldrich).

#### HepG2

HepG2 is an immortalized human hepatocellular carcinoma cell line, derived from a 15-year old Caucasian male. The cells were cultured in a T-75 culture flask in Gibco Dulbecco's Modified Eagle Medium (DMEM) (Lonza), containing 10% heat inactivated Fetal Bovine Serum, 1% L-glutamine (Lonza) and 1% Penicillin/Streptomycin (Lonza).

### 2.2 Induction of lipid droplets in hepatocytes

Lipid droplets are induced by adding PA (Cayman) and D-PA ( $d_{31}$ , Cayman) in 200 µM and 400 µM concentrations, dissolved in either ethanol or isopropanol. The 400 µM concentration is able to induce steatosis, without leading to a high amount of lipotoxicity [16]. Final solutions were created by diluting stock solutions of PA and D-PA in ethanol and isopropanol, by adding 1%-BSA medium, corresponding to the correct cell line.

### 2.3 Monolayer experiments

#### Alamar Blue Assay

To measure the metabolic activity of the cells, an Alamar Blue assay is performed. Resazurin, the active compound of Alamar Blue, is a non-fluorescent blue dye that can be reduced to resorufin, a high fluorescent pink color. This change can be induced by metabolically active cells.

Cells are seeded in a 24-well tissue-culture treated plate with a density of  $90 \times 10^3$  HepG2 cells per well and  $60 \times 10^3$  HepaRG cells per well. They are left to incubate at 37 °C for 24 hours. Then, the cells are treated with PA and D-PA in 200 µM and 400 µM concentrations, dissolved in both ethanol and isopropanol with controls of 200 µM and 400 µM of ethanol and isopropanol and a cell control with no treatment at all. The cells are incubated for 20 hours at 37 °C, after

---

<sup>1</sup>Note that when HepaRG cells are mentioned later on in this report, it refers to differentiated HepaRG cells.

which a 10% Alamar Blue solution was added to the cells. After incubating for 4-6 hours, the Alamar Blue solution was transferred to a black-based 96 well plate in duplo.

The fluorescent signal of the Alamar Blue solution in the black-based 96 well plate was measured using a VIKTOR™ plate reader. The results were presented as %-cell viability normalized to untreated control cells at 100%. When metabolic activity levels are 80% or higher compared to control cells, the cells are considered viable [2].

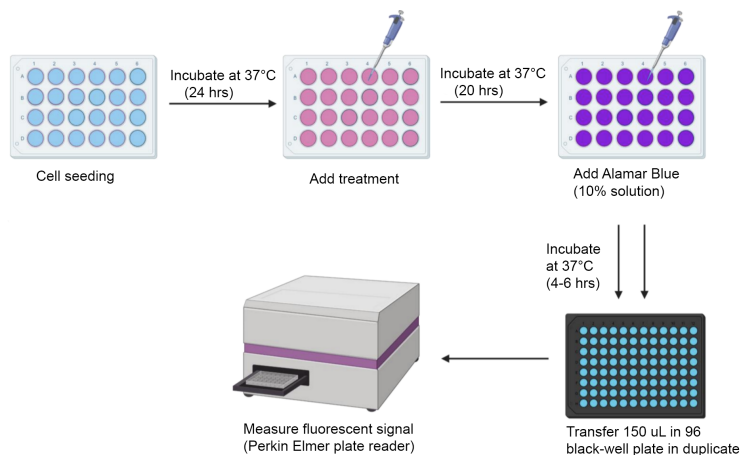


Figure 2.1: Alamar Blue assay protocol. [2]

### Oil-Red-O staining

Lipid accumulation was visualized with Oil-Red-O staining. Oil Red O is a fat-soluble dye used for staining of neutral lipids and TAGs, thereby visualizes fat droplets.

Cells were seeded in a 24-well tissue-culture treated plate with a density of  $50 \times 10^3$  HepG2,  $40 \times 10^3$  HepaRG cells per well. They were left to incubate at 37 °C for 24 hours. Then, the cells were treated with PA and D-PA in 200 uM and 400 uM concentrations, dissolved in both ethanol and isopropanol with controls of 200 uM and 400 uM of ethanol and isopropanol and a cell control with no treatment at all. The cells were once again incubated for 24 hours at 37 °C.

The cells were stained with Oil-Red-O following the manufacturers protocol. The nuclei were counterstained with haematoxylin, after which the cells were mounted using Aquatex.

### 2.4 Lipid droplet quantification

There are many ways to approach an attempt to quantify lipid droplets in histological images [17][18][19]. The most straightforward approach is to threshold a range of the digital color spectrum *RGB* (respectively red, green and blue). By carefully selecting different threshold values, it is possible to filter out all other colors except for the lipid droplets that are colored red due to the Oil-Red-O staining [20]. After the background is filtered out and all the LDs are left, an algorithm can analyze the droplets and calculate different properties of individual droplets such as size/area, location, roundness et cetera.

In this thesis, a method is developed to try and quantify lipid droplets in images of Oil-Red-O stained hepatocytes, treated with FAs and stained with Oil-Red-O. After the staining, the cells were imaged using a Nikon Eclipse Ti inverted microscope using an 18 MP CMOS camera. Six images per well (condition) were taken for quantification analysis at random spots in the well. Then, using MATLAB® with the Image Processing Toolbox™, an algorithm is developed which works in the following way:

1. Import batch of images from one experimental condition.
2. Use color thresholding on red, green and blue (RGB) channels to isolate lipid droplets and remove background.
3. Convert the thresholded image into binary, where the lipid droplets are white speckles and the background is black.
4. Use `bwlabel()` to label the lipid droplets and `regionprops()` to analyse the individual droplets.

The `regionprops()` function returns a structure array with properties of all the lipid droplets in the image. By calculating the size of this array, the amount of lipid droplets in an image can be determined. A lot of further information is available, i.e. the area, roundness and location of the lipid droplets in the image. In the first instance, only the amount of lipid droplets is taken into account.

A detailed description of the MATLAB®-script, used in analyzing the data, can be found in appendix A.

## 2.5 Spheroid formation

To create spheroids, cells were seeded in a Corning®Costar®Ultra-Low Attachment 96-well plate with a density of first 2000 cells per well and later 1000 cells for the HepG2/LX-2 spheroids and 2000 cells per well for the HepaRG/LX-2 spheroids, since HepG2 cells have a much higher proliferation rate and therefore result in larger spheroids.

To facilitate the compactness of the spheroids, the HepG2 and HepaRG cells were mixed with LX-2 cells. This is a hepatic stellate cell-line which gives the 3D structures a firmer shape, instead of the cells loosely hanging together. The mixing was done in a 24:1 ratio, the number 24 representing the HepaRG or HepG2 cell line. This specific ratio is known to be as close to the *in vivo* situation as possible [15]. 200 uL medium is added to the cells, also in a 24:1 ratio of HepG2/HepaRG medium to LX-2 medium, to facilitate the need of the cells. After 48 hours, treatment was added in duplo conditions by removing half of the volume in the wells and adding double concentrated treatment. This was done because not all medium can be removed without damaging the spheroid, so roughly 100 uL was left in the well.

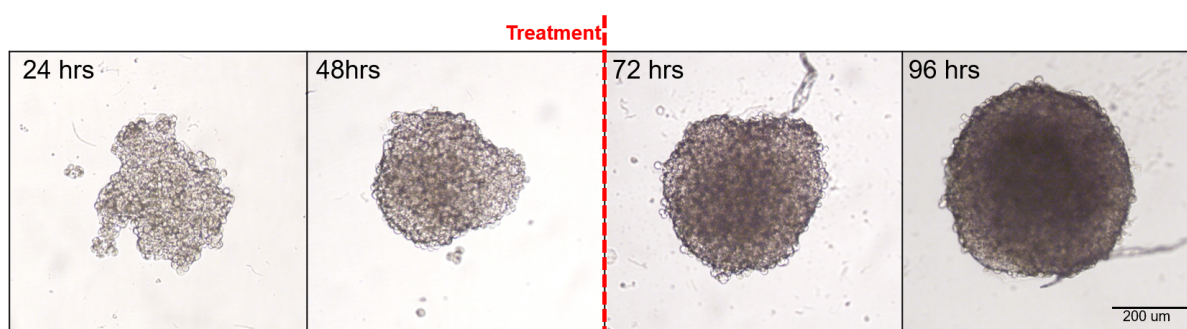


Figure 2.2: Spheroid formation of HepG2 and LX-2 cells in a respective 24:1 ratio. Treatment was added by removing half of the volume in the wells and adding double concentrated treatment to preserve spheroids. Images were taken after 24, 48, 72 and 96 hours after cell seeding.

### Oil-Red-O staining

There are different ways to perform Oil-Red-O structures on three-dimensional organoids. The most used approach is by culturing a 3D-structure and making slices by cryosectioning the

organoid [21] and then performing a histological (Oil-Red-O) staining. However, this approach is known to be very difficult and requires a lot of laboratory experience.

In this thesis, a much simpler way of performing an Oil-Red-O staining is done by sticking to the regular Oil-Red-O protocol and perform the stainings on the entire organoid. Small changes in this approach are made throughout the experiment, firstly to see if this method is any helpful and secondly to improve this way of staining organoids.

In general, two different protocols were tested. The first one uses microscope slides where the spheroids are transferred onto. Then, the staining was performed by very carefully adding and subtracting liquids from the microscope glass, after which the spheroids were mounted using Aquatex and a cover glass. The second approach requires the spheroids to be transferred into Eppendorf®-tubes. The staining was performed by carefully removing almost all medium and other liquids required by the protocol, then washing the spheroids two times with PBS after each step and then adding the next liquid to the spheroids. After the staining, the spheroids were transferred onto microscope slides after which they were mounted using Aquatex and a cover glass, just as before.

### **Alamar Blue assay**

It was not known how much incubation time was needed for the spheroids, since each individual spheroid contained very little cells ( $1 \times 10^3$  to  $2 \times 10^3$ ). After incubating for a little over 48 hours, a 10% Alamar Blue solution was added to the spheroids and medium controls. After incubating for about 5 hours, the Alamar Blue solution was carefully transferred to a black-based 96 well plate. In a later experiment, a 24 hour incubation time was used and the results were compared.

## 3 RESULTS AND DISCUSSION

### 3.1 Cellular metabolic activity

An Alamar Blue assay was used to indicate cell viability. The results are presented in figure 3.1 as a percentage of metabolic activity of the control cells. If cells under a certain condition are 100% metabolically active, it means that they are as active as the control (untreated) cells. A higher percentage means they are more active compared to control cells and vice versa. Normalizing against control cells makes it easier to compare the different cell lines to each other, since the proliferation rates are very different. Since HepG2 is a cancer cell line, the proliferation rate is much higher compared to the proliferation rate of HepaRG.

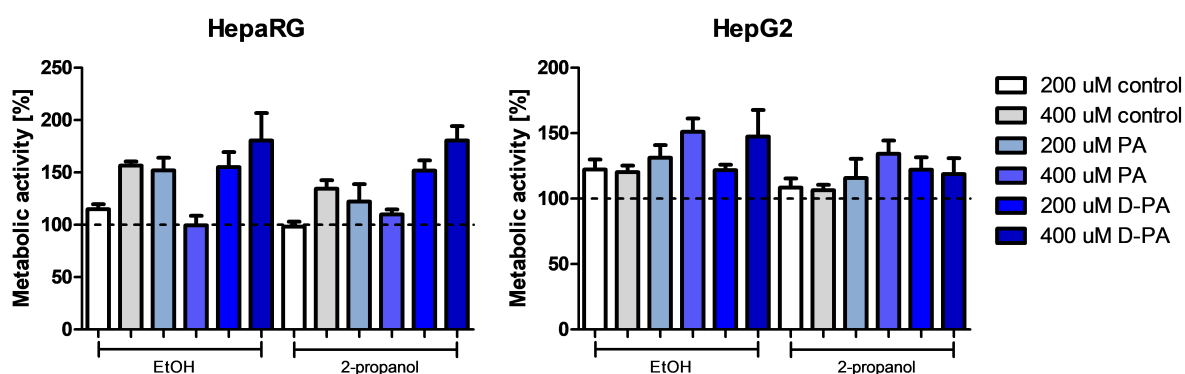


Figure 3.1: Results of the metabolic activity assay of the HepaRG (left) and HepG2 cell line (right). Metabolic activity is normalized against the cell control group (shown with a line at 100%). Presented are the averages of three experiments. Error bars are standard error of the mean.

#### 3.1.1 HepaRG metabolic activity

Looking at the dissolvent control groups, an increase of metabolic activity at higher molarities for both ethanol and isopropanol can be observed. This is also the case for D-PA. However, looking at PA, a decrease of metabolic activity at higher molarities of the fatty acid can be observed. There seems to be no trend difference between different dissolvents, while ethanol as a dissolvent seems to have a slightly higher overall metabolic activity compared to isopropanol. All the different experimental conditions resulted in at least 100% metabolic activity, normalized against untreated cells.

#### 3.1.2 HepG2 metabolic activity

In contrast to HepaRG cells, there seems to be no increase in metabolic activity at higher molarities of the dissolvent, looking at the dissolvent control groups. The addition of PA as well as

the addition of D-PA resulted in an increase in metabolic activity at higher molarities of the fatty acids in ethanol. In isopropanol however, there is also a slight increase of activity at increasing molarities of PA, but when looking at D-PA, no significant difference in activity can be observed. Similar to HepaRG cells, all conditions resulted in at least 100% metabolic activity.

### 3.1.3 Discussion of cellular metabolic activity

Although the error bars in figure 3.1 are higher compared to different studies ([2]), the general trend in increase or decrease of metabolic activity at different molarities using PA and D-PA on HepaRG cells is the same. The trends of different molarities of FAs shown in this thesis are slightly different from other studies (mentioned before), but that may be due to higher error bars on data used in this thesis.

High amounts of PA are known for their ability to induce lipotoxicity [22]. Previous studies ([22][2]) showed that HepaRG cells experience a drop in metabolic activity ( $\leq 80\%$ ) upon exposure of 400  $\mu\text{M}$  PA, although HepG2 cells seem to be more resistant to this phenomenon. However, looking at figure 3.1, this is not supported by this data since HepaRG cells remain metabolically active ( $\geq 80\%$ ) at 400  $\mu\text{M}$  of PA. However, it should be noted that metabolic activity of cells, when normalized against control cells, are peculiarly high. Other studies show an metabolic activity of around 100%, this data shows some metabolic activities well over 150%. Furthermore, the previous studies mentioned above showed much less variance in metabolic activity between different conditions than shown in figure 3.1. A possible explanation for this is lab handling inconsistencies of cells due to human error. The fluorescent signal induced by Alamar Blue is heavily dependent on the amount of Alamar Blue added to the medium of the cells, so a small deviation here may end up in large deviations in the fluorescent signal results.

## 3.2 Histological lipid droplet analysis

Lipid accumulation in HepaRG and HepG2 cells was visualized using Oil-Red-O stainings. Due to the properties of Oil Red O, lipid droplets can be visualized providing information about size, amount and distribution. Images of different conditions were taken and put into figures presented below. The experiment has been conducted three times, although only a fraction of the total images can be shown here. Only the most representative images have been presented, although all data has been taken into account when interpreting the results. Results are presented on the next pages, beginning with HepaRG and later HepG2 cells.

### 3.2.1 HepaRG

The results of the histological lipid droplet analysis are shown in figure 3.3 below. No lipid droplets were present in the control cells (figure 3.2) or dissolvent control cells. After treatment with both PA and D-PA, the formation of lipid droplets can be observed. There is no obvious difference visible between lipid droplets induced by PA or D-PA. At higher molarities, individual lipid droplet size did not seem to increase. However, higher molarities seem to result in a higher number of lipid droplets. Experiments were conducted with cells between passage number 10 and 14.

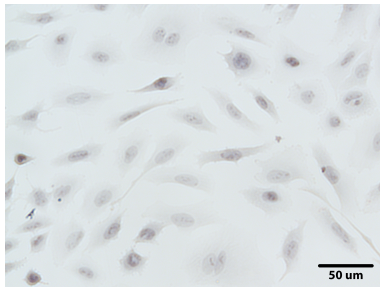


Figure 3.2: Control HepaRG cells after staining with Oil-Red-O. Adding no fatty acids or dissolvents resulted in no visible lipid droplets.

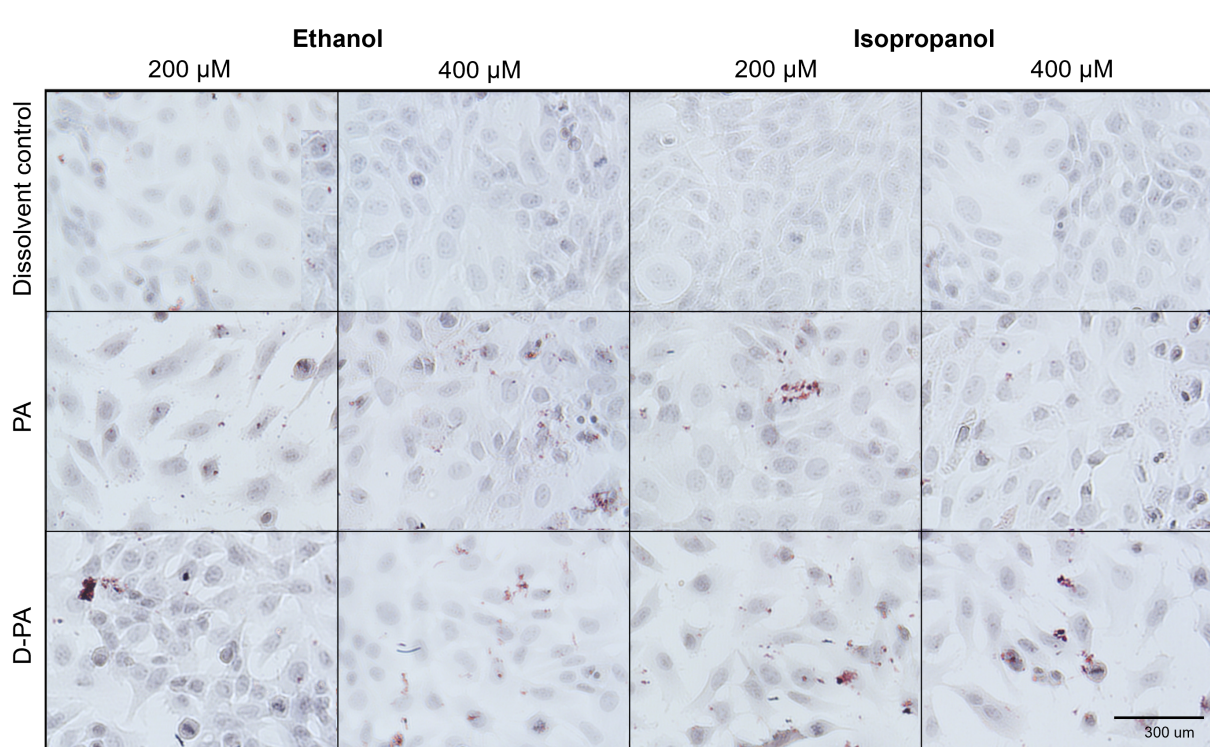


Figure 3.3: Results of Oil-Red-O staining of HepaRG cells. The first two columns show the ethanol groups at 200  $\mu$ M and 400  $\mu$ M, last two columns show the isopropanol groups at different molarities. The top row shows the dissolvent control groups, so the cells are not treated with fatty acids. The middle row shows cells treated with palmitic acid and the bottom row shows the cells treated with deuterated-palmitic acid.

### 3.2.2 HepG2

In contrast to HepaRG cells, both control (figure 3.4) and dissolvent control HepG2 cells already contain lipid droplets. After fatty acid treatment, the cells produced much more lipid droplets compared to the control cells. No difference between lipid droplets formed by PA or D-PA can be observed. Higher molarities increase lipid droplet amount as well as individual lipid droplet size. Experiments were conducted with passage number of cells between 50 and 54.

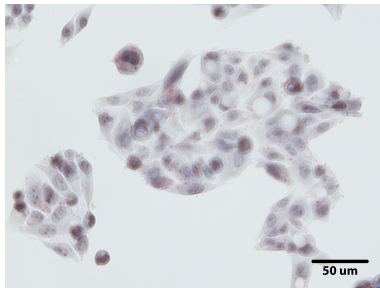


Figure 3.4: Control HepG2 cells after staining with Oil-Red-O. Adding no fatty acids or dissolvents already resulted in some small visible lipid droplets present.

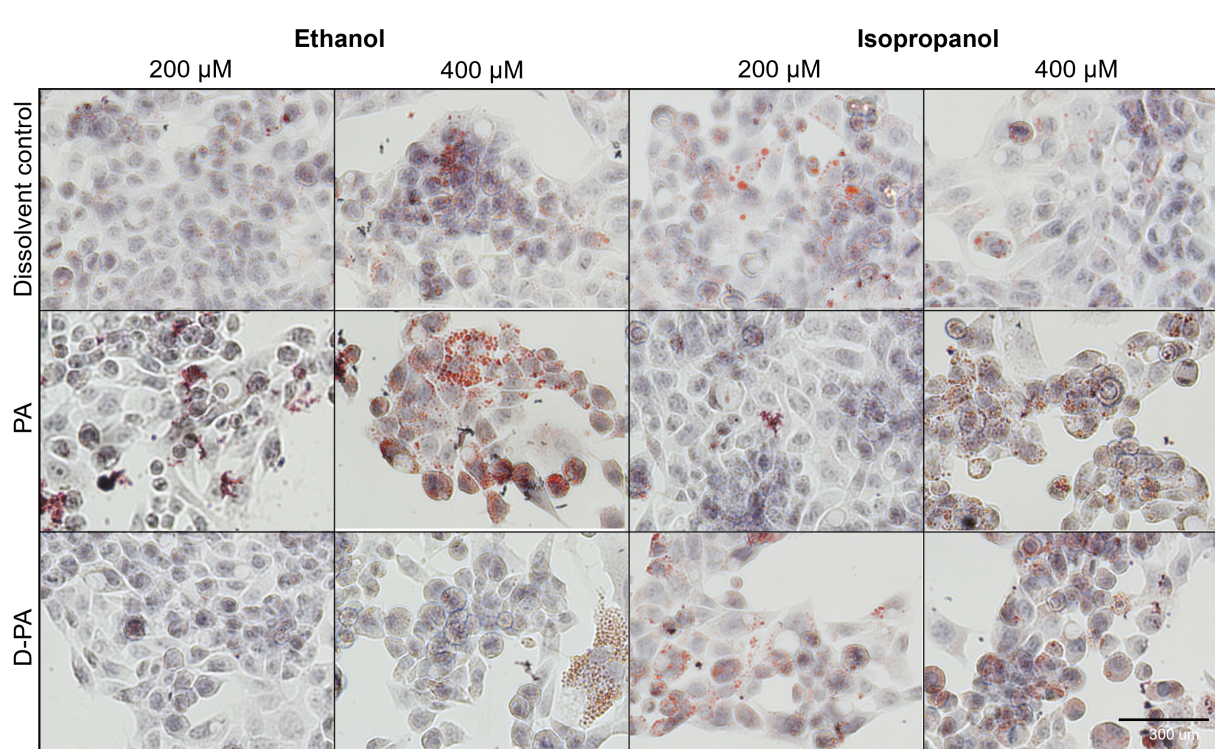


Figure 3.5: Results of Oil-Red-O staining of HepG2 cells. The first two columns show the ethanol groups at 200 uM and 400 uM, last two columns show the isopropanol groups at different molarities. The top row shows the dissolvent control groups, so the cells are not treated with fatty acids. The middle row shows cells treated with palmitic acid and the bottom row shows the cells treated with deuterated-palmitic acid.

### 3.2.3 Discussion

Note that these results and interpretations were done by visual examination. No quantification method has been applied yet; this will be examined in section 3.3.

#### **HepaRG**

Compared to HepG2 cells, HepaRG cells produced a lot less lipid droplets. A possible explanation for this is that the HepG2 cell line is a carcinoma cell line, making them much more metabolically active and therefore produce more lipid droplets when exposed to fatty acids.

#### **HepG2**

Compared to HepaRG cells, higher molarities of fatty acids seemed to increase individual droplet size. However, since HepG2 cells are known for their tendency to cluster together, this might also lead to lipid droplets in different cells sitting on top of each other, which leads to them seeming as one big droplet as opposed to multiple smaller ones.

### 3.3 Quantification of lipid droplets

Using a quantification algorithm made with MATLAB®, the images have been analyzed and the lipid droplets are quantified. The results are presented in this section.

Using six images per experimental condition, an average amount of LDs per condition was calculated. Since the experiment was conducted three times, the average of those three times were calculated and plotted in figure 3.6 below. Results are presented as a percentage of lipid droplets, normalized against the control cells. Below that, in figure 3.7, there are scatter plots of one out of the three experiments conducted under the same conditions. It is better to look at data from one experiment rather than three, since these plots contain absolute values and this is less comparable between experiments due to possible lab inconsistencies. The experiment chosen here is the best representative out of three.

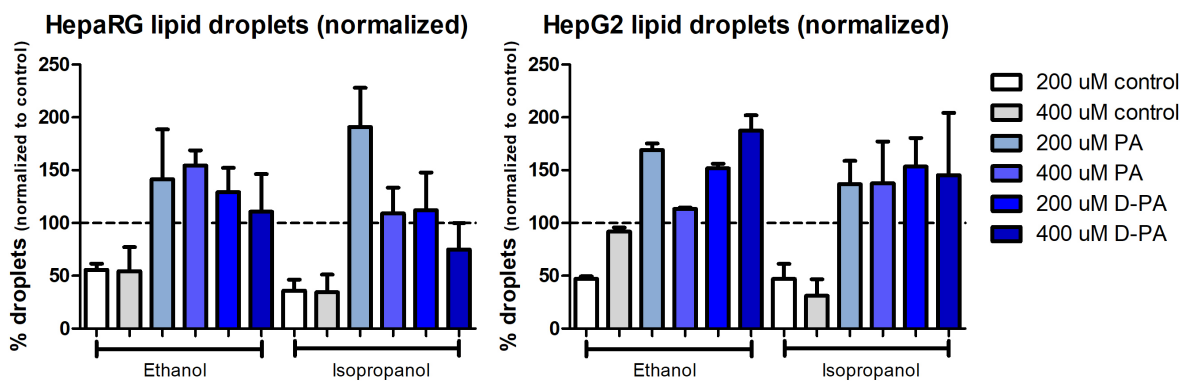


Figure 3.6: Results of quantification of the lipid droplets in HepaRG cells (left) and HepG2 cells (right) upon exposure of fatty acids. Results are normalized against the amount of droplets in control cells (with no treatment) and presented as a percentage. Error bars are standard error of the mean.

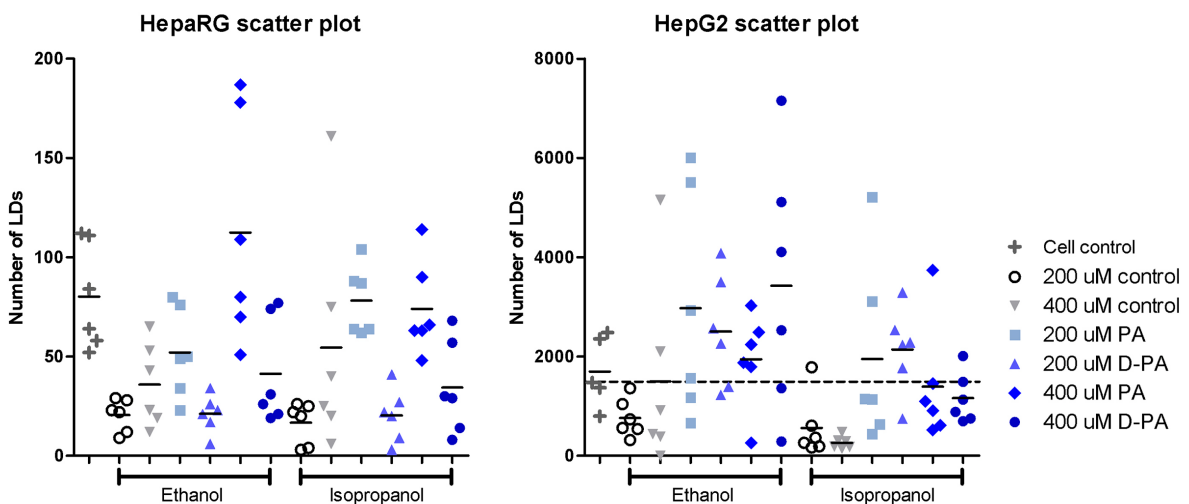


Figure 3.7: A scatter plot of the Oil-Red-O quantification data, gathered using MATLAB®. Data points contain a line at the mean.

#### HepaRG

Looking at HepaRG, a slight increase in LDs with higher molarities of PA can be seen when looking at ethanol as a dissolvent. Contrary to this, a slight decrease can be seen when looking

at D-PA in ethanol. When looking at isopropanol as a dissolvent of FAs, for both PA and D-PA a decrease of LDs can be observed at higher molarities. Both dissolvent controls stay consistent when increasing molarities.

### HepG2

Looking at HepG2, a reversed trend compared to HepaRG in ethanol can be observed as PA resulted in a decrease at higher molarities while D-PA resulted in more LDs at higher molarities. In isopropanol, the amount of LDs stayed fairly consistent at about 150% of the control cells.

### Additional data

Additional data was acquired from the master internship of student Gemma van der Sluijs [2]. HepaRG and HepG2 cells have been treated under the same conditions using the same protocols. This data is analyzed and presented the same way as mentioned before and used to extend the data acquired by this thesis.

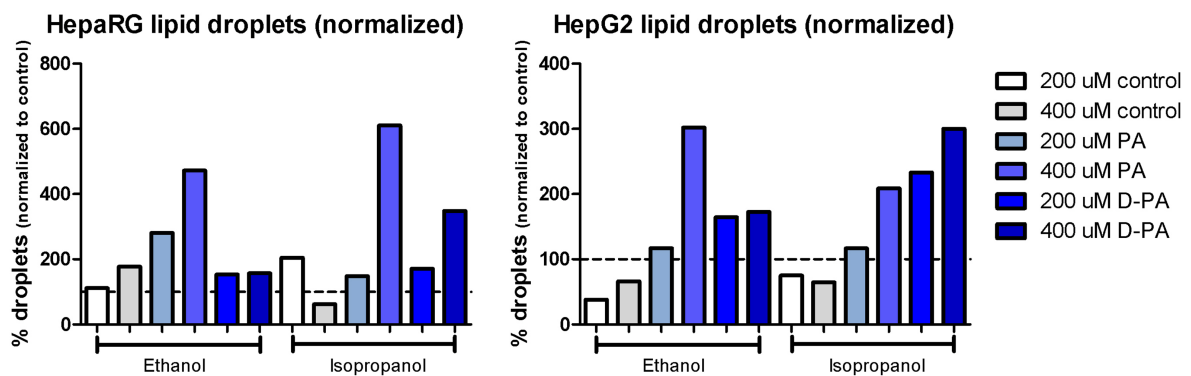


Figure 3.8: Results of quantification of additional data [2] of the lipid droplets in HepaRG cells (left) and HepG2 cells(right) upon exposure of fatty acids. Results are normalized against the amount of droplets in control cells (with no treatment) and presented as a percentage. Error bars are standard error of the mean

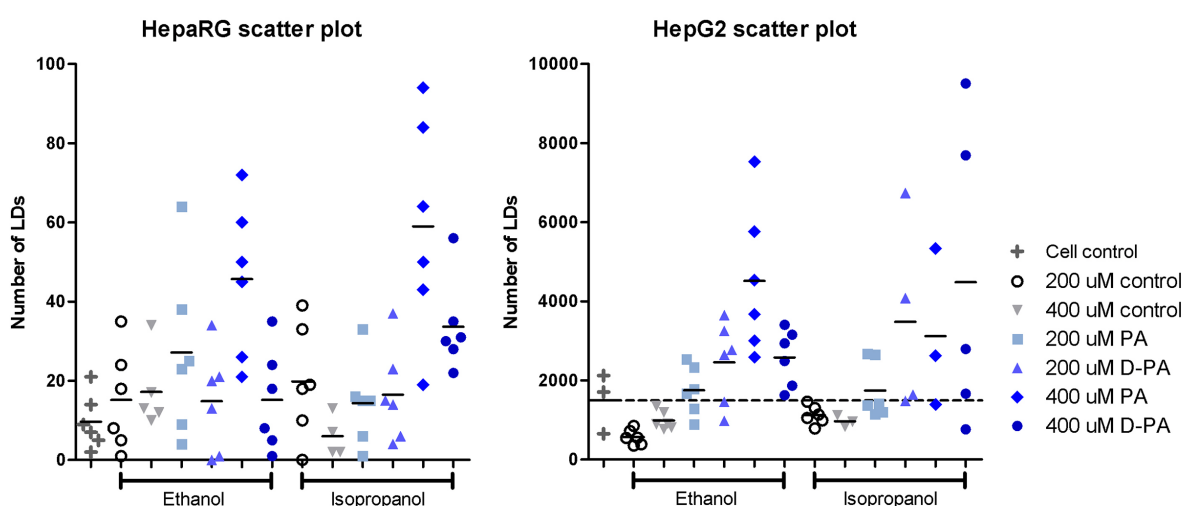


Figure 3.9: A scatter plot of the Oil-Red-O quantification of additional data [2], processed using MATLAB®. Data points contain a line at the mean.

### HepaRG

An increase in LDs at higher molarities can be seen when looking at PA in both dissolvents. In ethanol, D-PA remained the same and in isopropanol an increase in LDs can be observed. LDs in dissolvent controls seem to increase as the molarity goes up in ethanol and decrease in isopropanol.

### *HepG2*

The trend regarding to the different FAs are the same in HepG2 cells as in HepaRG cells. It either goes up or remains the same as the molarity increases. Dissolvent controls follow a similar trend.

## 3.3.1 Discussion of quantification

### **General**

There are a lot of possible improvements to make when it comes to the quantification method of LDs in hepatocytes, as used in this thesis. It is important that the image quality is as best as possible, to avoid any artifacts that could lead to false classifications as LDs. This influences the results since there are more LDs counted than actually present in the image. It is also critical that adequate color threshold values are used to only account for the red color of LDs. If boundaries are set too wide, objects in the images that are not LDs, are included in the quantifying process.

In the MATLAB®-script used in this thesis, only presumed LDs with an pixel-area equal to 1 are filtered out, since they cannot possibly be considered as LDs. However, this filtering is really basic and can be improved by implementing clever filtering techniques. Better filtering can be done by taking more information per individual LD into account by looking at area and roundness.

The amount of LDs varied a lot between images of the same experimental conditions. This is probably due to different cell densities throughout the wells. Although images are taken at six random spots in the well to account for systematic shortcomings, this can be improved by either taking more pictures or better distribute the cells during the plating protocol, where the cells are distributed throughout the well plate.

A possible explanation for large variances in results between experiments is the different color temperature of the light source used while acquiring the images. In processing the data, this has not been taken into account since the color threshold values were the same throughout processing all data from the experiments. These inconsistencies between experiments can also be explained by inconsistencies when following the Oil-Red-O staining protocol due to human error.

### **HepaRG**

HepaRG cells contained very little LDs compared to HepG2 cells. This means that artifacts and other deviations have, proportionally speaking, a much larger influence on the results. In some images, the naked eye could not spot any LDs although the MATLAB®-script counted a few dozen presumed LDs, possibly artifacts. Assuming the artifacts are about the same from image to image, normalizing the amount of LDs to the LDs in cell controls are thought to be an effective way to tackle this problem, or essentially reducing its influence.

### **HepG2**

Compared to HepaRG results, error bars on HepG2 results were significantly lower, especially when ethanol is used as a dissolvent. This is probably due to the proportionally smaller influence of artifacts on HepG2 results, since there are around a hundredfold more LDs per image.

### 3.4 Spheroid analysis

The cultured spheroids were analyzed using an Oil-Red-O staining and an Alamar Blue assay, as discussed in chapter 2.5.

#### 3.4.1 Histological analysis of spheroids

After staining the spheroids with Oil-Red-O, using different protocols (see chapter 2.5), the spheroids were transferred onto a microscope slide, mounted with Aquatex® and covered with a cover glass. Then, multiple images were taken at different imaging depths. One of the images is presented below (see figure 3.10).

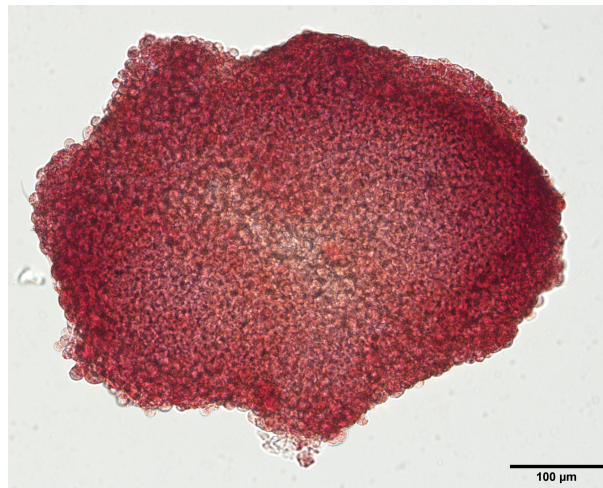


Figure 3.10: Oil-Red-O stained heterospheroid of HepG2 and LX-2 cells in a 24:1 ratio. 2000 cells were initially seeded. After 48 hours, the cells were treated with 200  $\mu$ M of D-PA, dissolved in ethanol.

There was no difference observable between spheroids treated with different conditions of fatty acids. Also, the control groups looked very similar to the spheroids treated with FAs. Overall, all spheroids look very red, despite the cell line used or different treatment conditions.

#### 3.4.2 Metabolic activity of spheroids

The results of the Alamar Blue assay on heterospheroids of HepaRG/LX-2 and HepG2/LX-2 cells are presented below in figure 3.11. Different incubation times after adding the 10% Alamar Blue solution of 6 hours and 24 hours are plotted. Each treatment condition was transferred to the black base 96-well plate in duplo before measurements were taken.

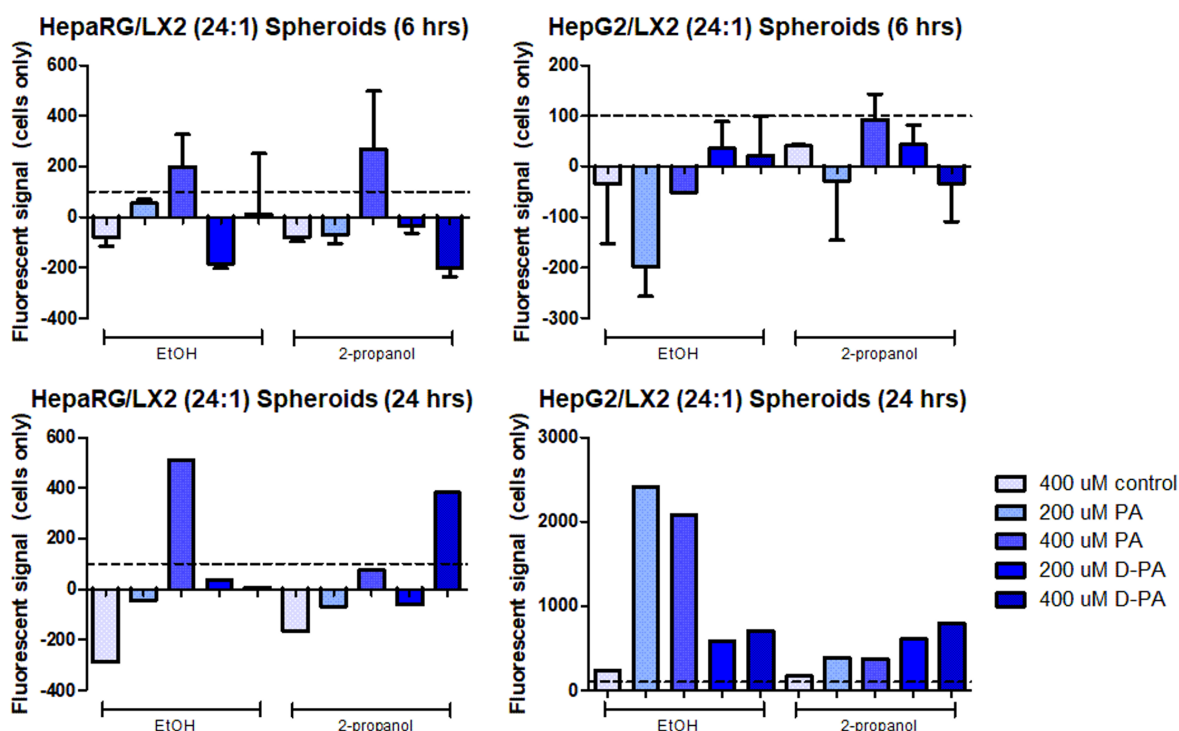


Figure 3.11: Results of Alamar Blue assay on heterospheroids. Note that y-axis displays fluorescent signal as measured by Viktor plate reader. Top row (n=2) shows results of HepaRG/LX-2 spheroids (left) and HepG2/LX-2 spheroids (right) after an Alamar Blue incubation time of 6 hours. Bottom row (n=1) shows the results after an incubation time of 24 hours.

### 3.4.3 Discussion of spheroid analysis

#### Oil-Red-O stainings

Despite different staining protocols, cell lines and treatment conditions, all spheroids looked very similar and very red. This is probably due to remnants of Oil-Red-O, which could not be properly washed away without damaging the spheroid and within reasonable time limits. Even when using more diluted solutions of Oil-Red-O and building in more washing steps in the protocol, results did not seem to change.

Due to the excessive amount of red spread all over the spheroids, these images could not be analyzed using the lipid droplet quantification algorithm as described in section 2.4.

**Alamar Blue assay** There was no significant difference between the fluorescent signal indicating the metabolic activity of the cells and the fluorescent signal of the medium controls. This indicates that the amount of cells present in the well were too low for this Alamar Blue analysis, since it is expected that the cells should have an impact on the fluorescent signal when compared to the control groups. Despite incubating the Alamar Blue solution for 24 hours instead of 6 hours, this did not give satisfying results that can indicate differences in metabolic activity that can be related to different treatment conditions.

## 4 CONCLUSION

The aim of this thesis was to visualize and quantify the size and distribution of LDs.

There seems to be a negative correlation between the metabolic activity and number of LDs present inside cells. Regardless of the cell line, dissolvent or isotope of FAs: when the number of LDs go up, the metabolic activity goes down.

Lipid droplets in the HepG2 cell line were bigger and present in higher numbers compared to the HepaRG cell line, although lipid droplets were already present in the control cells. Previous studies have shown that HepaRG cells are capable of forming more lipid droplets than in this thesis, but longer exposure time to FAs is needed.

Addition of FAs, regardless of isotope, dissolvent or molarity, almost always resulted in more LDs than the control cells. Dissolvent control cells resulted almost always in less LDs compared to the control cells. More lipid droplets were observed in higher molarities of fatty acids. Also, ethanol seems to be the better dissolvent since this resulted in a higher amount of lipid droplets. As expected, all lipid droplets are distributed throughout the cytoplasm, avoiding the nucleus.

As opposed to previous studies, no lipotoxicity was observed since all metabolic activities remained at least 100% or higher when compared to control cells, even upon exposure of 400  $\mu\text{M}$  of FAs. However, the metabolic activity did go down after the amount of LDs increased. It is expected to see metabolic activity values drop below 100% or even 80% when the concentration of FAs is further increased or if the same experiments are conducted under more strict conditions.

The amount of LDs formed upon exposure of PA was slightly higher than upon exposure of D-PA. This corresponds to the generally decreased metabolic activity of D-PA compared to PA and corresponds to the expectations due to the kinetic isotope effect. However, this does not mean that D-PA in Raman spectroscopy studies is unusable when analyzing the contents of lipid droplets.

The HepaRG cell line seems to be the better choice for NAFLD research since there are no lipid droplets present in the control cells. However, longer exposure times are needed to form more LDs. The HepG2 cell line is also capable of forming lipid droplets but since there are already lipid droplets present in control cells, it makes them less suitable for *in vitro* diagnostics of NAFLD studies. Furthermore, since the HepG2 cells tend to cluster together, this makes them harder to analyze, which would favor the HepaRG cells even more.

Spheroids proved to be very tricky when conducting experiments. The metabolic activity signals were too low to have any meaningful value since the amount of cells per well was very low. Even an incubation time of 24 hours rather than 4-6 hours did not give satisfying results. Furthermore, since there was no difference between treatment conditions observable and all the spheroids were colored very red, probably due to Oil-Red-O remnants, the results proved un-quantifiable using the created quantification algorithm.

## 5 FUTURE RESEARCH

It is important to improve the quantification method of LDs for use in future NAFLD studies. Thankfully, the method has much potential to improve and become more accurate. Better filtering, improved image quality and more (improved) data are relatively easy ways to advance this method of quantification.

It would be interesting to not only look at D-PA for the use of Raman spectroscopy in NAFLD studies, but also study the effect of other PA isotopes when hepatocytes are exposed to them. For instance,  $C_{16}$ -labeled PA is a lighter isotope compared to  $d_{31}$ -PA, so the kinetic isotope effect should slow the metabolism down to a lesser extent.

## Bibliography

1. Younossi ZM, Koenig AB, Abdelatif D, Fazel Y, Henry L, and Wymer M. Global epidemiology of nonalcoholic fatty liver disease—Meta-analytic assessment of prevalence, incidence, and outcomes. *Hepatology* 2016 Jul; 64:73–84. DOI: 10.1002/hep.28431
2. Sluijs G van der. Raman Spectral Imaging of Lipid Droplets in Human Hepatocytes in the Understanding of Non-Alcoholic Fatty Liver Disease. Tech. rep. University of Twente, 2021 Aug
3. Gluchowski NL, Becuwe M, Walther TC, and Farese RV. Lipid droplets and liver disease: from basic biology to clinical implications. *Nature Reviews Gastroenterology & Hepatology* 2017 Jun; 14:343–55. DOI: 10.1038/nrgastro.2017.32
4. Bruce A, Bray D, Johnson AD, Raff M, and Lewis J. *Essential Cell Biology*. 4th ed. W.W. Norton & Company, 2013 Nov
5. Zeng X, Zhu M, Liu X, Chen X, Yuan Y, Li L, Liu J, Lu Y, Cheng J, and Chen Y. Oleic acid ameliorates palmitic acid induced hepatocellular lipotoxicity by inhibition of ER stress and pyroptosis. *Nutrition & Metabolism* 2020 Dec; 17:11. DOI: 10.1186/s12986-020-0434-8
6. Ameer F, Scanduzzi L, Hasnain S, Kalbacher H, and Zaidi N. De novo lipogenesis in health and disease. *Metabolism* 2014 Jul; 63:895–902. DOI: 10.1016/j.metabol.2014.04.003
7. Nakagawa H, Hayata Y, Kawamura S, Yamada T, Fujiwara N, and Koike K. Lipid Metabolic Reprogramming in Hepatocellular Carcinoma. *Cancers* 2018 Nov; 10:447. DOI: 10.3390/cancers10110447
8. Marieb EN and Hoehn KN. *Human Anatomy and Physiology*. 10th ed. Pearson Education Limited, 2015
9. Mashek DG. Hepatic lipid droplets: A balancing act between energy storage and metabolic dysfunction in NAFLD. *Molecular Metabolism* 2021 Aug; 50:101115. DOI: 10.1016/j.molmet.2020.101115
10. Olzmann JA and Carvalho P. Dynamics and functions of lipid droplets. *Nature Reviews Molecular Cell Biology* 2019 Mar; 20:137–55. DOI: 10.1038/s41580-018-0085-z
11. Boden G. Obesity and Free Fatty Acids. *Endocrinology and Metabolism Clinics of North America* 2008 Sep; 37:635–46. DOI: 10.1016/j.ec1.2008.06.007
12. Engin AB. What Is Lipotoxicity? 2017 :197–220. DOI: 10.1007/978-3-319-48382-5{\\_}8
13. Malhi H, Bronk SF, Werneburg NW, and Gores GJ. Free Fatty Acids Induce JNK-dependent Hepatocyte Lipoapoptosis. *Journal of Biological Chemistry* 2006 Apr; 281:12093–101. DOI: 10.1074/jbc.M510660200
14. BIOPREDIC International. The HepaRG Cell Line. Available from: <https://www.heparg.com/rubrique-the-heparg-cell-line#>
15. Pingitore P, Sasidharan K, Ekstrand M, Prill S, Lindén D, and Romeo S. Human multi-lineage 3D spheroids as a model of liver steatosis and fibrosis. *International Journal of Molecular Sciences* 2019 Apr; 20. DOI: 10.3390/ijms20071629
16. Gómez-Lechón MJ, Donato MT, Martínez-Romero A, Jiménez N, Castell JV, and O'Connor JE. A human hepatocellular in vitro model to investigate steatosis. *Chemico-Biological Interactions* 2007 Jan; 165:106–16. DOI: 10.1016/j.cbi.2006.11.004

17. Biltz NK and Meyer GA. A novel method for the quantification of fatty infiltration in skeletal muscle. *Skeletal Muscle* 2017 Jan; 7. DOI: 10.1186/s13395-016-0118-2
18. Exner T, Beretta CA, Gao Q, Afting C, Romero-Brey I, Bartenschlager R, Fehring L, Popelreuther M, and Füllekrug J. Lipid droplet quantification based on iterative image processing. *Journal of Lipid Research* 2019; 60:1333–44. DOI: 10.1194/jlr.D092841
19. Nault R, Colbry D, Brandenberger C, Harkema JR, and Zacharewski TR. Development of a Computational High-Throughput Tool for the Quantitative Examination of Dose-Dependent Histological Features. *Toxicologic Pathology* 2015; 43:366–75. DOI: 10.1177/0192623314544379
20. Deutsch MJ, Schriever SC, Roscher AA, and Ensenauer R. Digital image analysis approach for lipid droplet size quantitation of Oil Red O-stained cultured cells. *Analytical Biochemistry* 2014; 445:87–9. DOI: 10.1016/j.ab.2013.10.001
21. Vidavsky N, Kunitake JAMR, Diaz-Rubio ME, Chiou AE, Loh HC, Zhang S, Masic A, Fischbach C, and Estroff LA. Mapping and Profiling Lipid Distribution in a 3D Model of Breast Cancer Progression. *ACS Central Science* 2019 May; 5:768–80. DOI: 10.1021/acscentsci.8b00932
22. Alsabeeh N, Chausse B, Kakimoto PA, Kowaltowski AJ, and Shirihai O. Cell culture models of fatty acid overload: Problems and solutions. *Biochimica et Biophysica Acta (BBA) - Molecular and Cell Biology of Lipids* 2018 Feb; 1863:143–51. DOI: 10.1016/j.bbalip.2017.11.006

## A OIL-RED-O QUANTIFICATION USING MATLAB

```
1 % Stan Wissink
2 % 15 December 2021
3
4 clc; clear all; close all;
5
6 rawMeasurements = [];
7 numberOfDroplets = [];
8
9 N = 6; % <-- Number of images per condition
10
11 Name= "Visual result comparison";
12
13 for i = 1 : N
14     % use the filename
15     fi = sprintf('%d.bmp', i);
16     originalImage = imread(fi);
17     originalGray = rgb2gray(originalImage);
18
19     Binary = createMask(originalImage);
20     BinaryFill = imfill(Binary, 'holes');
21
22     % Visual examination
23     subplot(2,6,i), imshow(originalImage), title(i + ": Original");
24     subplot(2,6,i+N), imshow(BinaryFill), title(i + ": Binary");
25     set(gcf, 'units', 'normalized', 'outerposition', [0 0 1 1]);
26
27     labeledImage = bwlabel(BinaryFill, 8);
28
29     rawMeasurements{i} = regionprops(labeledImage, originalGray, 'Area');
30     cellRaw = struct2cell(rawMeasurements{1,i})';
31     idx = cellfun(@(x) isequal(x,1), cellRaw(:,1));
32     filteredMeasurements{i} = cellRaw( idx, :);
33
34     numberOfDroplets(i) = size(filteredMeasurements{1,i}, 1);
35 end
36
37 numberOfDroplets %%ok<NOPTS>
38
39 savefig(Name); % Save the figure of visual comparison between original image and
40
41 function [BW,maskedRGBImage] = createMask(RGB)
42 % Convert RGB image to chosen color space
43 I = RGB;
44 % Define thresholds for channel 1 based on histogram settings
45 channel1Min = 0.000;
46 channel1Max = 255.000;
47 % Define thresholds for channel 2 based on histogram settings
48 channel2Min = 0.000;
49 channel2Max = 100.000;
```

```

50 % Define thresholds for channel 3 based on histogram settings
51 channel3Min = 0.000;
52 channel3Max = 100.000;
53 % Create mask based on chosen histogram thresholds
54 sliderBW = (I(:,:,1) >= channel1Min ) & (I(:,:,1) <= channel1Max) & ...
55     (I(:,:,2) >= channel2Min ) & (I(:,:,2) <= channel2Max) & ...
56     (I(:,:,3) >= channel3Min ) & (I(:,:,3) <= channel3Max);
57 BW = sliderBW;
58 % Initialize output masked image based on input image.
59 maskedRGBImage = RGB;
60 % Set background pixels where BW is false to zero.
61 maskedRGBImage(repmat( BW,[1 1 3])) = 0;
62 end

```